Journal of Achievements in Materials and Manufacturing Engineering
VOLUME 52
ISSUE 2
June
2012

Investigations of nanocrystalline and gradient coatings produced by cathodic arc evaporation technology

K. Lukaszkowicz*
Division of Materials Processing Technology, Management and Computer Techniques in Materials Science, Institute of Engineering Materials and Biomaterials, Silesian University of Technology, ul. Konarskiego 18a, 44-100 Gliwice, Poland
* Corresponding e-mail address: krzysztof.lukaszkowicz@polsl.pl

Received 12.04.2012; published in revised form 01.06.2012

Materials

ABSTRACT

Purpose: The main aim of the this research was the investigation of the microstructure, corrosion resistance and the mechanical properties of the nanocrystalline TiAlSiN, CrAlSiN, AlTiCrN and the gradient TiAlN, TiCN, AlSiCrN coatings deposited by cathodic arc evaporation technology onto the X40CrMoV5-1 hot work tool steel substrate.
Design/methodology/approach: The surfaces' topography and the microstructure of the investigated coatings were observed on the scanning electron microscopy. Diffraction and thin film structure were tested with the use of the transmission electron microscopy. The microhardness tests were made on the dynamic ultra-microhardness tester. Tests of the coatings' adhesion to the substrate material were made using the scratch test.
Findings: It was found that the microstructure of the nanocrystalline coatings consisted of fine crystallites, while their average size fitted within the range of 11-25 nm, depending on the coating type. The critical load L_{C2} lies within the range of 46-54 N. In case of the gradient coatings it was found that the microstructure consisted of crystallites while their average size fitted within the range of 25-50 nm, depending on the coating type. The coatings demonstrated columnar structure as well as good adhesion to the substrate. The critical load L_{C2} lies within the range 46-59 N. The coatings demonstrate a high hardness (40 GPa) and corrosion resistance.
Practical implications: In order to evaluate with more detail the possibility of applying these surface layers in tools, further investigations should be concentrated on the determination of the thermal fatigue resistance of the coatings. The very good mechanical properties of the nanocrystalline and gradient coatings make them suitable in industrial applications.
Originality/value: The investigation results will provide useful information to applying the nanocrystalline and gradient coatings for the improvement of mechanical properties of the hot work tool steels.
Keywords: Thin and thick coatings; Nanocrystalline coatings; Gradient coatings; Microstructure; Mechanical properties

Reference to this paper should be given in the following way:
K. Lukaszkowicz, Investigations of nanocrystalline and gradient coatings produced by cathodic arc evaporation technology, Journal of Achievements in Materials and Manufacturing Engineering 52/2 (2012) 75-82.

1. Introduction

For several decades, tool material designers have been trying to develop and produce an ideal tool material of high ductility and maximum possible wear resistance characteristics in working conditions. Such combination is practically impossible to obtain. Therefore, various attempts were made to find at least a partial solution to the issue, by creation of layer structures, the methods included without limitation of thermal-chemical treatment, composite material production and monolayer or multilayer coating deposition by the CVD and PVD methods as well as overlaying welding or hard layer spraying by the spray metallization method [1-5].

The research issues concerning the production of coatings is one of the more important directions of surface engineering development, ensuring the obtainment of coatings of high usable properties in the scope of mechanical characteristics and wear resistance. The progress in the field of producing coatings in the physical vapour deposition process enables the obtainment of coatings of nanocrystal structure presenting high mechanical and usable properties. The coatings of such structure are able to maintain a low friction coefficient in numerous working environments, maintaining high hardness and increased resistance [6, 7]. The main concept in the achievement of high hardness of nanostructure coatings and good mechanical properties and high strength related to it, particularly in case of nanocomposite coatings is the restriction of the rise and the movement of dislocations [8-11]. Nanocomposite coatings comprise at least two phases, a nanocrystalline phase and a matrix phase, where the matrix can be either nanocrystalline or amorphous phase [12, 13].

Functional gradient coatings create a new class of coatings with properties and structure changing gradually. Gradient coatings deposited on the tool material substrate and providing appropriately high resistance to abrasive wear in tool operating conditions, core ductility and stress relaxation between the particular coating layers and between the gradient coating and tool material coating are seen as a solution to the issue due to the inappropriate adhesion of the layer produced or the excessive stresses between the surface layer and the substrate [14, 15]. Frequently a rapid difference between the coating and substrate properties occurs causing a stress concentration in this area, both during the manufacturing and operation of the tools. This causes fast degradation demonstrated by cracks and delamination of the coatings. The application of functional gradient coatings offers a possible solution to the issue. Gradient coatings can be applied in manufacturing modern machining tools, due to their resistance to high-temperature oxidation and erosion as well as abrasive wear [16,17].

The purpose of this paper is to examine the microstructure, mechanical properties and corrosion resistance of nanocrystalline and gradient coatings deposited by PVD technique on the X40CrMoV5-1 hot work tool steel substrate.

2. Investigation methodology

The tests were made on samples of the X40CrMoV5-1 hot work tool steel deposited by PVD process with TiAlSiN, CrAlSiN, AlTiCrN nanocrystalline coatings and TiAlN, TiCN, AlSiCrN gradient coatings. The coating deposition process was made in a device based on the cathodic arc evaporation method in an Ar, C_2H_2 and N_2 atmosphere. Cathodes containing pure metals (Cr, Ti) and the AlSi (88:12 wt.%) alloy were used for deposition of the coatings. The base pressure was 5×10^{-6} mbar. The deposition conditions are summarized in Tables 1 and 2.

Specimens were subjected to heat treatment consisting in quenching and tempering; austenizing was carried out in the vacuum furnace at 1020°C with a soaking time of 0.5 h. Two isothermal holds were used during heating up to the austenizing temperature, the first at the temperature of 640°C and the second at 840°C. The specimens were tempered twice after quenching, each time for 2 hours at the temperature of 560°C and next at 510°C. To ensure a proper quality, the surfaces of the steel specimens have been subjected to mechanical grinding and polishing (R_a=0.03 μm).

Observations of surface and structures of the deposited coatings were carried out on cross sections in the SUPRA 35 scanning electron microscope. Detection of secondary electron was used for generation of fracture images with 15 kV bias voltage.

Diffraction and thin film structure were tested with the use of the JEOL JEM 3010UHR transmission electron microscope, at 300 kV bias voltage. Thin foils were made by mechanical grinding and further ion polished using the Gatan apparatus.

Phase identification of the investigated coatings was performed by glancing angle X-ray diffraction (GAXRD).

The cross-sectional atomic composition of the samples was obtained by using a glow discharge optical spectrometer, GDOS-750 QDP from Leco Instruments. The following operation conditions of the spectrometer Grimm lamp were fixed during the tests:

- lamp inner diameter-4 mm;
- lamp supply voltage-700 V;
- lamp current-20 mA;
- working pressure-100 Pa.

Tests of the coatings' adhesion to the substrate material were made using the scratch test on the CSM REVETEST device. The tests were made using the following parameters:

- load range: 0-100 N,
- load increase rate (dL/dt): 100 $Nmin^{-1}$,
- indenter's sliding speed (dx/dt): 10 $mmmin^{-1}$,
- acoustic emission detector's sensitivity AE: 1.

The critical load L_C, causing the loss of the coating adhesion to the material, was determined on the basis of the values of the acoustic emission, AE, and friction force, F_t, and observation of the damage developed in the track using a LEICA MEF4A optical microscope.

X-ray line broadening technique was used to determine crystallite size of the coatings using Scherrer formula with silicon as internal standard:

$$D = (0.9\lambda/B\cos\theta_B)$$

where:
D - crystallite size,
B - full width at half-maximum XRD peak in radians,
λ - wavelength of the X-ray radiation,
θ_B - the Bragg angle in radians.

Table 1.
Deposition parameters of the nanocrystalline coatings

Coating	Substrate bias voltage,V	Arc current source, A	Temperature, °C	Pressure, Pa
TiAlSiN	-90	Ti - 80 AlSi - 120	450	2.0
CrAlSiN	-60	Cr - 70 AlSi - 120	450	3.0
AlTiCrN	-60	Cr - 70 AlTi - 120	450	2.0

Table 2.
Deposition parameters of the gradient coatings

Coating	Substrate bias voltage, V	Arc current source, A	Temperature, °C	Gas mixture	
				Nitrogen flow rate, sccm	Acetylene flow rate, sccm
TiAlN	-60	TiAl - 60	350	100→250	-
AlSiCrN	-60	Cr - 60 AlSi - 60	350	100→250	-
TiCN	-60	Ti - 60	500	250→100	0→200

The microhardness tests of coatings were made with the SHIMADZU DUH 202 ultra-microhardness tester. The test conditions were selected in order as to be comparable for all coatings. Measurements were made with 50 mN load, to eliminate the substrate influence on the coating hardness.

The thickness of coatings was determined using the ''kalotest'' method, i.e. measuring the characteristics of the spherical cap crater developed on the surface of the coated specimen tested.

Investigation of the electrochemical corrosion behaviour of the samples was done in a PGP 201 Potentiostat/Galvanostat, using a conventional three-electrode cell consisting of a saturated calomel reference electrode (SCE), a platinum counter electrode, and the studied specimens as the working electrode. To simulate the aggressive media, a HCl 1M solution was used under aerated conditions and room temperature. The aqueous corrosion behavior of the coatings was studied first by measuring the open circuit potential (OCP) for 1h. Subsequently, a potentiodynamic polarization curve has been recorded. The curve started at a potential of approx. 100 mV below the corrosion potential and ended at +1200 mV or a threshold intensity level set at 100 mA/cm^2. Once this level was reached, the reverse cycle was started. The scan rate was 15 mV/min. The corrosion current densities and the polarization resistance were obtained on the basis of the Tafel analysis after potentiodynamic polarization measurements.

3. Discussion of results

The nanocrystalline coatings present a compact structure, without any visible delaminations or defects. The morphology of the fracture of coatings is characterized with a dense structure, in some cases there is a columnar structure (Figs. 1, 2). The fractographic studies of the fractures of the steel samples examined, with the coatings deposited on their surface show a sharp transition zone between the substrate and the coating. The gradient coatings' structure appears to be compact without any visible delamination or defects. The investigated coatings tested show a columnar structure that may be considered compatible with the Thornton model (zone I), except the fact that in TiCN the cross-section morphology is dense (Figs. 3, 4).

Transmission electron microscopy (TEM) examination of the nanocrystalline coatings showed that they consisted of fine crystallites, of average size ca. 11-25 nm, depending on the kind of coating (Fig. 5). Single large grains were only observed in case of the TiAlSiN coating, which may suggest the occurrence of the epitaxion phenomenon as the consequence of large crystallite occurrence in the coating. The gradient TiAlN and TiCN coating observations in the TEM (Fig. 6) indicate that such coatings consists of fine crystallites, of average size ca. 25-50 nm, depending on the kind of coating. Generally, there are no foundations to confirm the epitaxial growth of the investigated coatings. Several large grains were observed in the AlSiCrN coating and the possibility of epitaxy due to the presence of large crystalites may be deduced upon examination of the SAED pattern.

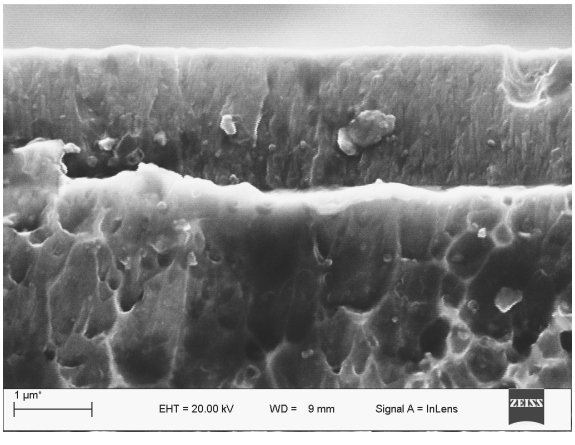

Fig. 1. Fracture of the nanocrystalline TiAlSiN coating deposited onto the X40CrMoV5-1 steel substrate

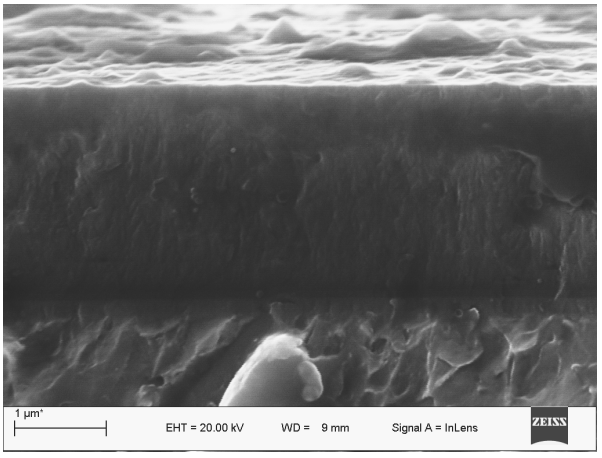

Fig. 2. Fracture of the nanocrystalline CrAlSiN coating deposited onto the X40CrMoV5-1 steel substrate

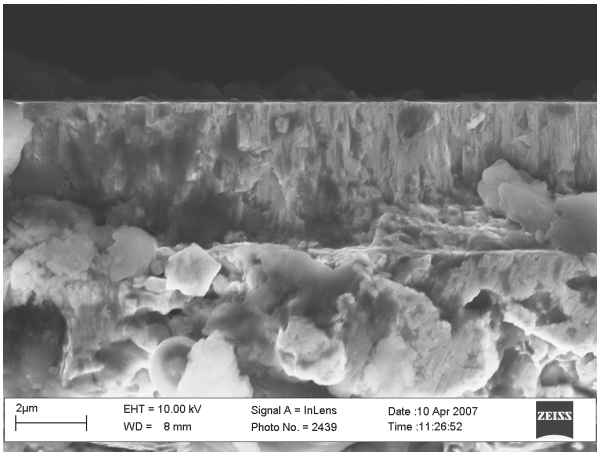

Fig. 3. Fracture of the gradient TiAlN coating deposited onto the X40CrMoV5-1 steel substrate

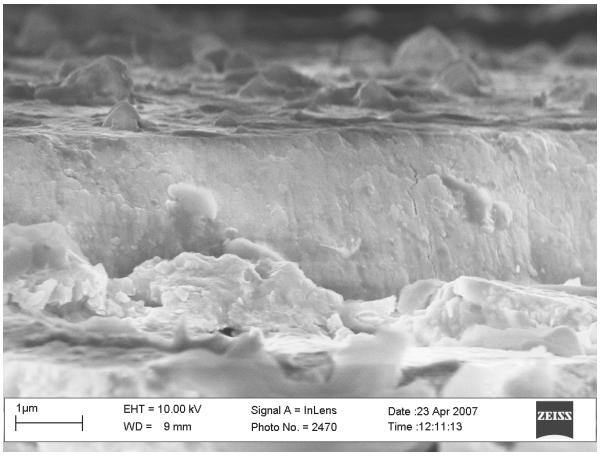

Fig. 4. Fracture of the gradient TiCN coating deposited onto the X40CrMoV5-1 steel substrate

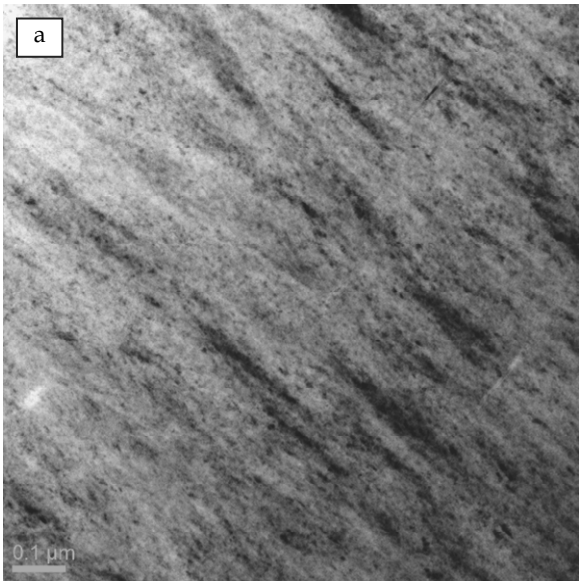

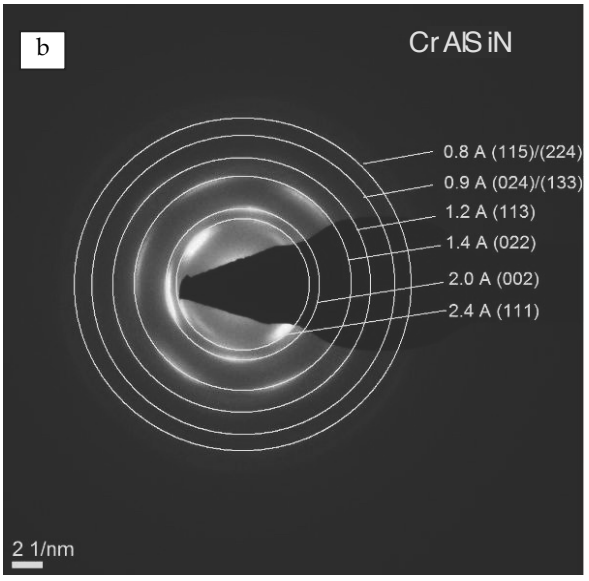

Fig. 5. a) Structure of the thin foil from the nanocrystalline CrAlSiN coating deposited onto the hot work tool steel X40CrMoV5-1, b) diffraction pattern from the area as in figure a and solution of the diffraction pattern

Basing on the glancing angle X-ray diffraction (GAXRD) of the samples examined (Fig. 7), the occurrence of fcc phases was only observed in the coatings. The hexagonal AlN of wurtzite type was not discovered in the coatings examined, which could have been caused by a low amount of aluminium in the coatings. In case of the TiAlSiN coating a lattice parameter of 0.426 nm was derived, which is greater than that of bulk TiN (0.424 nm). The highest lattice parameter corresponds to a system where a partial Si segregation occurred, which might be enough to nucleate and develop a Si_3N_4 amorphous phase. Also, decrease

intensities of the reflections, showing an increase in the amorphous content in the coatings. Basing on the results obtained, using Scherer method, the size of crystallites in the coatings examined was determined. The results were presented in Table 3.

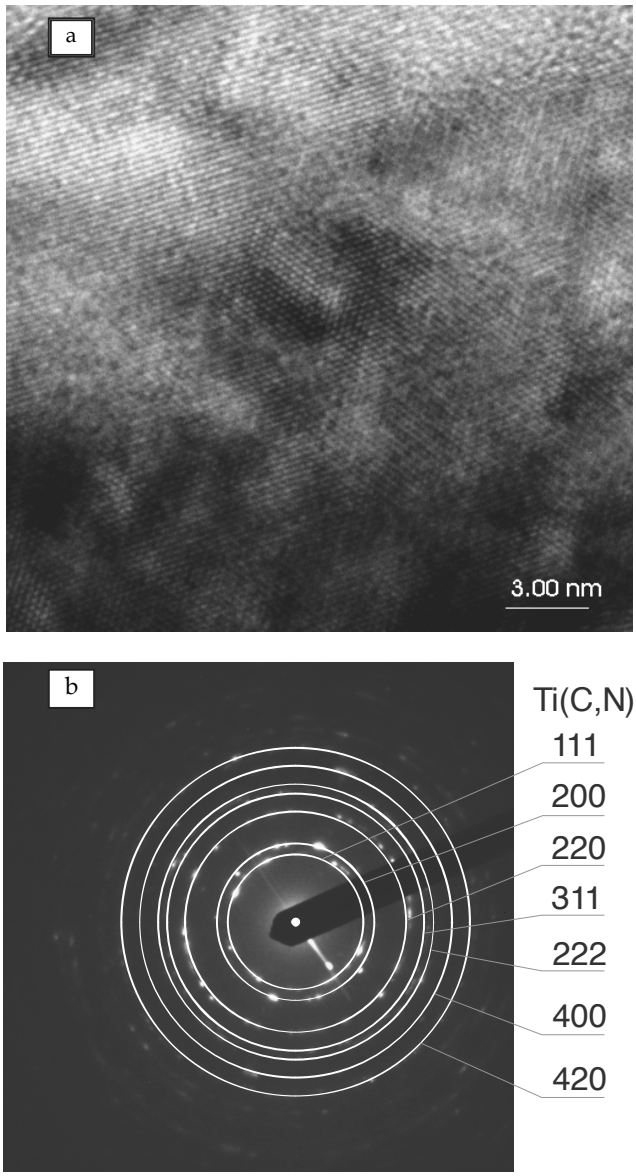

Fig. 6. a) Structure of the thin foil from the gradient TiCN coating deposited onto the hot work tool steel X40CrMoV5-1, b) diffraction pattern from the area as in figure a and solution of the diffraction pattern

The hardness of the X40CrMoV5-1 steel substrate without coating is 2.1 GPa, as settled upon hardness tests. The deposition of the PVD coatings onto the specimens causes the growth of hardness of the surface layer ranging from 30 to 32 GPa in case of gradient coatings and from 36 to 40 GPa in case of nanocrystalline coatings (Table 3).

The critical load values L_{C1} and L_{C2} were determined by the scratch test method (Figs. 8, 9). The load at which the first coating defects appear is known in the references as the first critical load L_{C1}. The first critical load L_{C1} corresponds to the point at which first damage is observed; the first appearance of microcraking, surface flaking outside or inside the track without any exposure of the substrate material - the first cohesion-related failure event. L_{C1} corresponds to the first small jump on the acoustic emission signal, as well as on the friction force curve. The second critical load L_{C2} is the point at which complete delamination of the coatings starts; the first appearance of cracking, chipping, spallation and delamination outside or inside the track with the exposure of the substrate material - the first adhesion-related failure event. After this point the acoustic emission graph and friction forces have a disturbed run (become noisier). The cumulative specification of the test results are presented in Table 3. In order to establish the nature of damage responsible for the occurring increase of the acoustic emission intensity, the cracks produced during the test were examined by the light microscope coupled with the measuring device, determining the critical load L_{C1} and L_{C2} in virtue of metallographic observations. In case of the nanocrystalline coatings examined, it was found that coating AlTiCrN had the highest critical load value L_{C1}=24 N and L_{C2}=54 N. In case of the gradient coatings examined, it was found that the TiCN coating had the highest critical load of L_{C1} = 33 and L_{C2} = 59 N, whereas AlSiCrN and the TiAlN coatings had the lowest L_{C1} = 19 and L_{C2} = 46 N. The TiCN coatings show the best adhesion to the substrate of all the gradient coatings tested, which is not only due to the adhesion itself, but also due to mixing of the elements in the transition zone between the coating and the substrate as a result of diffusion, because the TiCN coatings' deposition process temperature was 500°C.

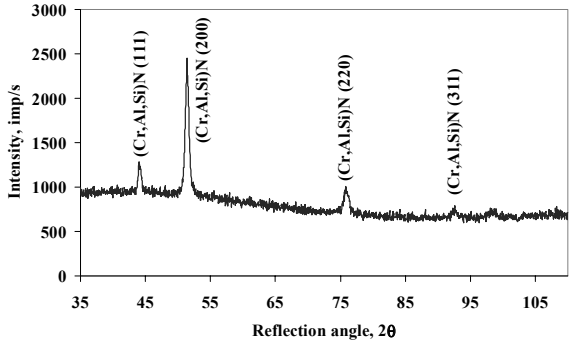

Fig. 7. GAXRD spectra of the nanocrystalline CrAlSiN coating at glancing incidence angle α=2°

Changes of coating component concentration and substrate material made in GDOS were presented in Figs. 10, 11. The tests carried out with the use of GDOS indicate the occurrence of a transition zone between the substrate material and the coating, which results in the improved adhesion between the coatings and the substrate. In the transition zone between the coatings and the substrate the concentration of the elements of the substrate increases with simultaneous rapid decrease of concentration of elements contained in the coatings.

Table 3.
The characteristics of the tested coatings

Coating	Thickness, μm	Microhardness, GPa	Crystallite size, nm	Critical load L_{C1}, N	Critical load L_{C2},N
Nanocrystalline coatings					
AlTiCrN	2.4	38	17	24	54
CrAlSiN	2.9	40	25	18	49
TiAlSiN	2.1	36	11	16	46
Gradient coatings					
TiAlN	2.8	32	25	19	46
AlSiCrN	2.1	32	34	25	46
TiCN	4.2	30	50	28	59

a) b)

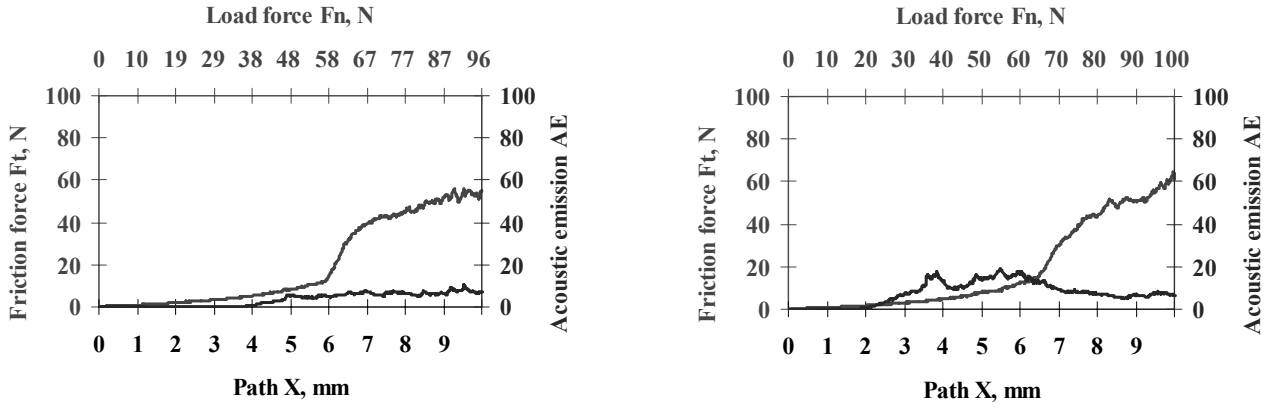

Fig. 8. Diagram of the dependence of the acoustic emission (AE) and friction force F_t on the load for the X40CrMoV5-1 steel with the: a) AlTiCrN, b) TiAlSiN coating

a) b)

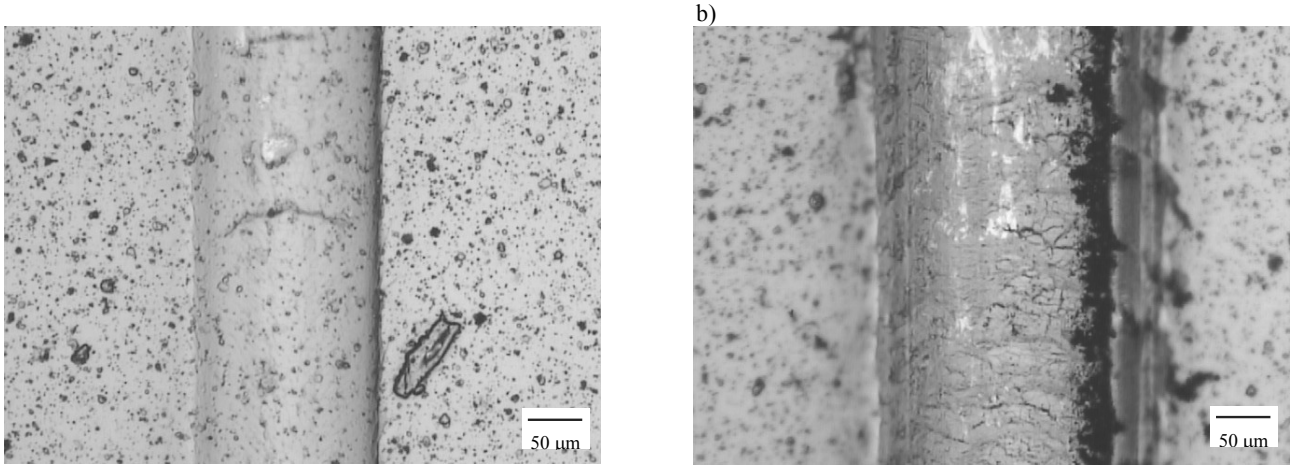

Fig. 9. Scratch failure pictures of the AlTiCrN coating on X40CrMoV5-1 steel substrate at: (a) L_{C1}, (b) L_{C2}

The existence of the transition zone should be connected with the increase of desorption of the substrate surface and the occurrence of defects in the substrate and the relocation of the elements within the connection zone as a result of a high energy ion reaction. Such results, however, cannot be interpreted explicitly, due to the non-homogeneous evaporation of the material from the sample surface.

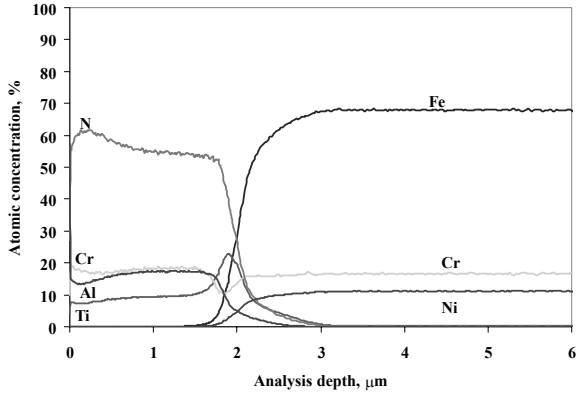

Fig. 10. Changes of constituent concentration of the nanocrystalline AlTiCrN coating and the substrate materials

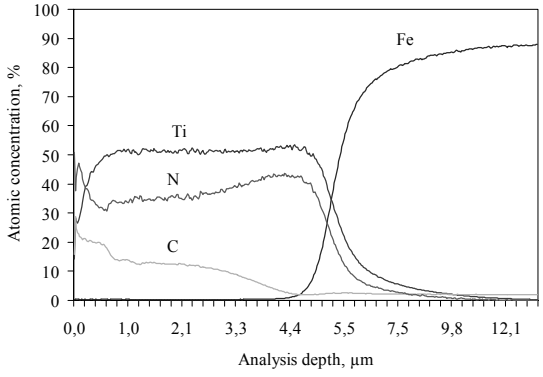

Fig. 11. Changes of constituent concentration of the gradient TiCN coating and the substrate materials

As a result of tests on the electrochemical corrosion, it was observed that the coatings deposited by PVD process on the substrate made of theX40CrMoV5-1 steel constitute effective protection of the substrate material against the corrosive affect of the aggressive factor. The potentiodynamic polarisation curve analysis (Figs. 12, 13) and that of the corrosion rate confirm the better corrosion resistance of the samples with coatings layers in comparison to the uncovered sample. During the anode scanning the current density is always lower for the sample with a coating deposited on its surface in comparison to the uncovered sample (11.56 μAcm^{-2}), which indicates a good protective effect. The potentiodynamic polarisation curve course is the evidence of the active process of the uncoated steel surface. The lowest corrosion current density of the investigated coatings are obtained (from Tafel plot) for the nanocrystalline CrAlSiN coating. This can be explain by the relatively low porosity of this coating. The current density for the other coatings is significantly higher than the one obtained for the CrAlSiN coating. The curve course in the cathodic range indicates a strong inhibition of the reactions taking place on coated steel. The behaviour of the systems tested within the anodic range may evidence the porosity or defect of the coatings. Some of the coatings tested within the anodic range were subjected to self-passivation, however, the passive state occurs within a narrow range of the potentials. The growth of the anodic current related to the transpassivation was observed within the 0-0.4 mV potential range. The corrosion current density and corrosion rate were estimated according to the potentiodynamic curve courses. The corrosion potential E_{cor} test results confirm the better corrosive resistance of the coatings in comparison to the uncoated steel samples. The fact that the corrosive potential of the uncoated substrate significantly grows after a 60-minute experiment is also worth noting.

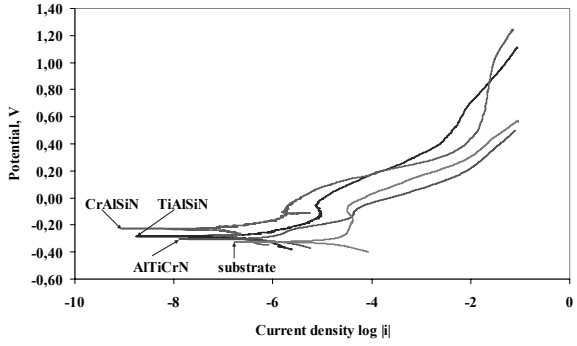

Fig. 12. Potentiodynamic polarization curves of the nanocrystalline coatings in 1 M HCl solution

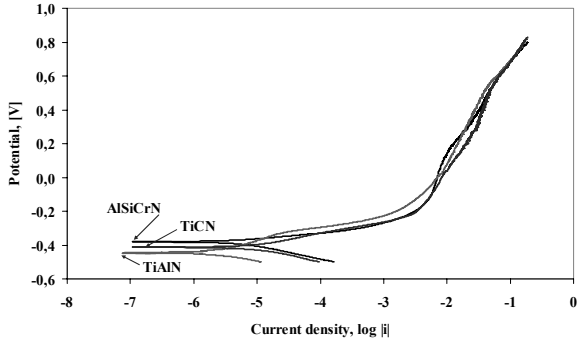

Fig. 13. Potentiodynamic polarization curves of the gradient coatings in 1 M HCl solution

4. Summary

In case of nanocrystalline coatings the compact structure of the coatings without any visible delaminations was observed as a result of tests in the scanning electron microscope. The fracture morphology of the coatings tested is characterised with a dense structure. Basing on the thin film test in the transmission electron

microscope, it was observed that the coatings are built of fine crystallites. Their size is 11-25 nm. The coating adhesion scratch tests disclose the cohesion and adhesion properties of the coatings tested. In virtue of the tests carried out, it was found that the critical load L_{C2} fitted within the range 46-54 N for the coatings deposited on a substrate made of hot work tool steel. The tests made with the use of GDOS indicate the occurrence of a transition zone between the substrate material and the coating, which affects the improved adhesion between the coatings and the substrate. As a result of the potentiodynamic polarisation curve analysis, the corrosion current density - corrosion rate was determined. It confirms the better corrosion resistance of samples coated with the use of the PVD technique to the uncoated samples made of the austenitic steel (11.65 μAcm^{-2}). The corrosion current density for the coatings tested fits within the range 0.15-0.77 μAcm^{-2}, which proves their good anti-corrosion properties.

In case of gradient coatings the compact structure of the coatings without any visible delamination was observed in the scanning electron microscope. The investigated TiAlN and CrAlSiN coatings show columnar structure, which may be considered compatible with the Thornton model (zone I). Upon examination of the thin films obtained from TiAlN and TiCN coatings, it was found that the coatings were composed of fine crystallites. The scratch tests on coating adhesion the reveal the cohesive and adhesive properties of the coatings deposited on the substrate of the X40CrMoV5-1 hot work tool steel. On the basis of the above examinations, it was found that the critical load of L_{C2} is between 46-59 N. The biggest value of the critical load was obtained for the TiCN coating. The GDOS investigations indicate the existence of the transition zone between the substrate material and the coating resulting in the improved adhesion of the coatings deposited to the substrate.

Acknowledgements

Research was financed partially within the framework of the Polish State Committee for Scientific Research Project No N N507 550738 headed by Dr Krzysztof Lukaszkowicz.

References

[1] L.P. Karpov, Use of double thermochemical treatment in the production of tools from structures steels, Materials Science and Heat Treatment 45/1-2 (2003) 8-9.
[2] L.A. Dobrzański, K. Lukaszkowicz, A. Križ, Properties of the multi-layer Ti/CrN and Ti/TiAlN coatings deposited with the PVD technique onto brass substrate, Journal of Materials Processing Technology 143 (2003) 832-837.
[3] L.A. Dobrzański, E. Jonda, K. Lukaszkowicz, A. Križ, Structure and tribological behavior of surface layer of laser modified X40CrMoV5-1 steel, Journal of Achievements in Materials and Manufacturing Engineering 18/1-2 (2006) 343-346.
G. Matula, K. Gołombek, J. Mikuła, L.A. Dobrzański, Structure of sintered gradient tool materials, Journal of Achievements in Materials and Manufacturing Engineering 32/1 (2009) 23-28.
[4] K. Lukaszkowicz, L.A. Dobrzański A. Zarychta, Structure, chemical and phase compositions of coatings deposited by reactive magnetron sputtering onto the brass substrate, Journal of Materials Processing Technology 157 (2004) 380-387.
[5] K. Lukaszkowicz, J. Konieczny, Microstructure and mechanical properties of PVD nanocrystalline layers, Solid State Phenomena 186 (2012) 230-233.
[6] K. Lukaszkowicz, A. Kriz, J. Sondor, Structure and adhesion of thin coatings deposited by PVD technology on the X6CrNiMoTi17-12-2 and X40CrMoV5-1 steel substrates, Archives of Materials Science 51/1 (2011) 40-47.
[7] K. Lukaszkowicz, Review of nanocomposite thin films and coatings deposited by PVD and CVD technology, In: Nanomaterials, Mohammed Muzibur Rahman (Ed.), Intech, Rijeka, 2011, 145-162.
[8] S.M. Yang, Y.Y. Chang, D.Y. Wang, D.Y. Lin, W.T. Wu, Mechanical properties of nano-structured Ti-Si-N film synthesized by cathodic arc evaporation, Journal of Alloys and Compounds 440 (2007) 375-379.
[9] K. Lukaszkowicz, L.A. Dobrzański, W. Kwaśny, K. Labisz, M. Pancielejko, Microstructure and mechanical properties of nanocomposite coatings deposited by cathodic arc evaporation, Journal of Achievements in Materials and Manufacturing Engineering 42 (2010) 156-163.
[10] K. Lukaszkowicz, L.A. Dobrzański, J. Sondor, Microstructure, mechanical properties and corrosion resistance of nanocomposite coatings deposited by PVD technology, In: Advances in diverse industrial applications of nanocomposites, Boreddy S.R. Reddy (Ed.), Intech, Rijeka, Croatia, 2011, 1-16.
[11] S. Veprek, S. Reiprich, A concept for the design of novel superhard coatings, Thin Solid Films 268 (1995) 64-71.
[12] S. Veprek, Conventional and new approaches towards the design of novel superhard materials, Surface and Coatings Technology 97 (1997) 15-22.
[13] I. Dahan, U. Admon, N. Frage, J. Sariel, M.P. Dariel, J.J. Moore, The development of a functionally graded TiC-Ti multilayer hard coatings, Surface and Coatings Technology 137 (2001) 111-115.
[14] U. Schulz, M. Peters, F.W. Bach, G. Tegeder, Graded coatings for thermal, wear and corrosion barriers, Materials Science and Engineering 362 (2003) 61-80.
[15] L.A. Dobrzański, M. Staszuk, A. Križ, K. Lukaszkowicz, Structure and mechanical properties of PVD gradient coatings deposited onto tool steels and sialon tool ceramics, Journal of Achievements in Materials and Manufacturing Engineering 37/1 (2009) 36-43.
[16] K. Lukaszkowicz, L.A. Dobrzański, M. Pancielejko, Mechanical properties of the PVD gradient coatings deposited onto the hot work tool steel X40CrMoV5-1, Journal of Achievements in Materials and Manufacturing Engineering 24/2 (2007) 115-118.